The tubulin cofactor C family member TBCCD1 orchestrates cytoskeletal filament formation

Jane André[1], Stephanie Harrison[1,*], Katie Towers[2], Xin Qi[1], Sue Vaughan[2], Paul G. McKean[1,†] and Michael L. Ginger[1,†]

[1]Faculty of Health and Medicine, Division of Biomedical and Life Sciences, Lancaster University, Lancaster LA1 4YQ, UK
[2]Oxford Brookes University, Gipsy Lane, Oxford OX3 0BP, UK

*Present address: Paterson Institute for Cancer Research, The University of Manchester, Manchester M20 4BX, UK
†Authors for correspondence (p.mckean@lancaster.ac.uk; m.ginger@lancaster.ac.uk)

Accepted 9 September 2013
Journal of Cell Science 126, 5350–5356

doi: 10.1242/jcs.136515

Summary

TBCCD1 is an enigmatic member of the tubulin-binding cofactor C (TBCC) family of proteins required for mother–daughter centriole linkage in the green alga *Chlamydomonas reinhardtii* and nucleus–centrosome–Golgi linkage in mammalian cells. Loss of these linkages has severe morphogenetic consequences, but the mechanism(s) through which TBCCD1 contributes to cell organisation is unknown. In the African sleeping sickness parasite *Trypanosoma brucei* a microtubule-dominant cytoskeleton dictates cell shape, influencing strongly the positioning and inheritance patterns of key intracellular organelles. Here, we show the trypanosome orthologue of TBCCD1 is found at multiple locations: centrioles, the centriole-associated Golgi 'bi-lobe', and the anterior end of the cell body. Loss of *Trypanosoma brucei* TBCCD1 results in disorganisation of the structurally complex bi-lobe architecture and loss of centriole linkage to the single unit-copy mitochondrial genome (or kinetoplast) of the parasite. We therefore identify TBCCD1 as an essential protein associated with at least two filament-based structures in the trypanosome cytoskeleton. The last common ancestor of trypanosomes, animals and green algae was arguably the last common ancestor of all eukaryotes. On the basis of our observations, and interpretation of published data, we argue for an unexpected co-option of the TBCC domain for an essential non-tubulin-related function at an early point during evolution of the eukaryotic cytoskeleton.

Key words: Cytoskeleton, Golgi, Kinetoplast, Tubulin-binding cofactor C, TBCC domain, TBCCD1, Trypanosome

Introduction

Tubulin cofactor C (TBCC) interacts with other tubulin cofactors to stimulate the GTPase activity of β-tubulin to release α-tubulin–β-tubulin heterodimers competent for microtubule incorporation (Tian et al., 1996). Human XRP2 (a TBCC-domain containing protein mutated in certain forms of retinitis pigmentosa – a retinal degenerative disease) is proposed to act as GTPase-activating protein (GAP) for protein(s) other than tubulin, albeit in a cytoskeletal context (Veltel et al., 2008; Schwarz et al., 2012). In canonical TBCC and XRP2, stimulation of GTPase activity is dependent upon a catalytic arginine residue (Bartolini et al., 2002). TBCCD1 is an enigmatic TBCC family member. In the green alga *Chlamydomonas reinhardtii*, TBCCD1 is found associated with the centrioles and rhizoplasts (fibres that connect centrioles to the nucleus; Brugerolle and Mignot, 2003). In *Chlamydomonas*, centrioles are multifunctional and are involved in both axoneme formation and mitotic spindle organisation. In the absence of TBCCD1 defects in centriole number, centriole positioning and mitotic spindle organisation are seen (Feldman and Marshall, 2009). In animal cells, TBCCD1 is required for centrosome–Golgi linkage (Gonçalves et al., 2010), but in both *Chlamydomonas* and animal cells how TBCCD1 serves its function is unknown. At first glance, the presence of a TBCC domain suggests that GAP activity is intrinsic to TBCCD1 function. However, TBCCD1 lacks the obvious catalytic arginine of TBCC and XRP2, although in their alignment of TBCCD1, XRP2 and TBCC orthologues Feldman and Marshall (Feldman and Marshall, 2009) identified an arginine residue nearby. The authors speculated this arginine could suffice for GAP activity and suggested that TBCCD1 might function in processing tubulin, including atypical centriole-associated δ- and ε-tubulin. However, other amino residues within the TBCC domain that are conserved in TBCC and RP2, and that are probably crucial for catalytic function (Kühnel et al., 2006), are not conserved in TBCCD1 despite a prediction of conserved secondary structure (our unpublished observations; see Materials and Methods). Moreover, whereas TBCC and XRP2 partially complement the yeast *CIN2* (TBCC) deletion mutant (Bartolini et al., 2002), TBCCD1 cannot (Gonçalves et al., 2010). Thus the role of TBCCD1 as a GAP is questionable. *Trypanosoma brucei* is the aetiological agent of African sleeping sickness, but, from a cell biology perspective, cell form is governed by an elaborate microtubule-based cytoskeleton in which centrioles (or basal bodies) are the template for axoneme formation (Portman and Gull, 2012) but mitosis is closed and occurs independently of centriole involvement (Ogbadoyi et al., 2000). Here, we reveal trypanosome TBCCD1 is an essential protein that functions in diverse aspects of filament-based cell biology with no evident role in microtubule organisation.

Results and Discussion

Centriolar, Golgi-associated bilobe, and anterior cell end localisations for *T. brucei* TBCCD1

To localise *T. brucei* TBCCD1 (*Tb*TBCCD1; encoded by Tb927.11.2440 and identified as a TBCCD1 orthologue in Feldman and Marshall, 2009), we expressed the protein fused to the C-terminus of yellow fluorescent protein (^{Ty}YFP:TBCCD1). Using a pENT-based vector system (Kelly et al., 2007), recombinant gene expression occurred from an endogenous chromosomal locus under the control of native *cis*-acting elements. Visualisation of ^{Ty}YFP:TBCCD1 at early stages of the cell division cycle (1K1N) revealed several foci of YFP fluorescence: (1) close to the kinetoplast (an elaborate concatenation of ~5000 DNA circles forming the trypanosome mitochondrial genome; Jensen and Englund, 2012), (2) at an elongate structure immediately anterior to the kinetoplast, and (3) at the anterior end of the cell body (Fig. 1A). This pattern was retained in detergent-extracted cytoskeletons, indicating tight cytoskeletal association. To look further at localisation and determine the temporal order of signal duplication, we stained detergent-extracted cytoskeletons for indirect immunofluorescence using antibodies recognising various cytoskeletal structures (Fig. 1B–I). Monoclonal antibody YL1/2 recognises a pool of tyrosinated α-tubulin at transitional fibres located at the distal end of the mature basal body (Stephan et al., 2007) and monoclonal antibody BBA4 recognises an antigen from the proximal ends of both mature and pro-basal bodies (Woods et al., 1989). In dual-fluorescence experiments, two ^{Ty}YFP:TBCCD1 foci were positioned more proximally to the kinetoplast than YL1/2, but distal to antigen recognised by BBA4 (Fig. 1B,C). Thus, one pool of ^{Ty}YFP:TBCCD1 coincides with the microtubule barrels of mature and pro-basal bodies.

The *T. brucei* flagellum is attached to the cell body for most of its length via the flagellum attachment zone (FAZ). Monoclonal antibody L3B2 recognises FAZ1 protein from the cytoplasmic face of the FAZ (Vaughan et al., 2008). In trypanosomes with one flagellum, and which are therefore at either the start or the end of their cell division cycle, L3B2 immunofluorescence revealed ^{Ty}YFP:TBCCD1 immediately adjacent to the distal end of the FAZ signal, consistent with recruitment of ^{Ty}YFP:TBCCD1 to the anterior end of the cell body (Fig. 1D). Careful analysis of cells at various stages of the cell division cycle revealed the new 'anterior end' signal did not track with the new FAZ that elongates during new flagellum assembly. Rather, new signal appeared during mitosis; duplication occurred early in mitosis and the duplicated signal (Fig. 1E, arrowed) was acquired prior to full FAZ maturation (as defined by L3B2 labelling). At the anterior end of trypanosome cells, the minus ends of microtubules forming the sub-pellicular corset are clustered (Sherwin and Gull, 1989); duplication of the anterior end ^{Ty}YFP:TBCCD1 signal potentially marks the site for cleavage furrow ingression, which initiates at this point during cytokinesis (Fig. 1F).

Position and appearance of the elongate ^{Ty}YFP:TBCCD1 signal adjacent to basal bodies was immediately reminiscent of the trypanosome-specific filamentous 'bi-lobe' (Esson et al., 2012) implicated in providing a template for cell-cycle-regulated Golgi biogenesis and duplication in *T. brucei* (Ho et al., 2006). Fluorescence and immunoelectron microscopy of known bi-lobe proteins, including centrin isoforms and various trypanosomatid-specific proteins, reveal the bi-lobe to possess a complex sub-structure (Esson et al., 2012; Gheiratmand et al., 2013; Morriswood et al., 2013). Immunofluorescence with either the monoclonal pan-centrin antibody 20H5 (Fig. 1G) or cyan fluorescent protein (CFP)-tagged to the bi-lobe protein *Tb*MORN (CFP:MORN) (Fig. 1H) confirmed *Tb*TBCCD1 as a novel bi-lobe component. However, *Tb*TBCCD1 did not localise fully to either of two known bi-lobe sub-structures: the 'fishhook' denoted by *Tb*MORN or the centrin-containing bi-lobe arm as described by Esson et al. and Morriswood et al. (Esson et al., 2102; Morriswood et al., 2013). Immunofluorescence with polyclonal antiserum recognising the Golgi marker RabX2 (Natesan et al., 2009) confirmed the presence of the Golgi stack adjacent to the *Tb*TBCCD1-containing bi-lobe (Fig. 1I). Expression of *Tb*TBCCD1 fused at its C-terminus to GFP (TBCCD1:GFP^{Ty}) gave an identical pattern of fluorescence to ^{Ty}YFP:TBCCD1. Signal amplification using anti-YFP antibodies failed to detect further ^{Ty}YFP:TBCCD1 foci at any point in the cell cycle. Crucially, given the lethal RNAi phenotype described below, cells expressing only TBCCD1:GFP^{Ty} or ^{Ty}YFP:TBCCD1 grew without discernible morphological defects. The illustrations in Fig. 2 summarise the localisation of *Tb*TBCCD1 to three distinct sites within trypanosomes, and also indicate the timing of signal duplications during the cell division cycle.

Morphogenetic failures in *Tb*TBCCD1 RNAi lines

Loss of 'bi-lobe' organisation

To probe *Tb*TBCCD1 function we induced RNA interference (RNAi) in cells expressing ^{Ty}YFP:TBCCD1. Following RNAi induction, retardation of the growth rate and reduction in *Tb*TBCCD1 protein levels occurred (Fig. 3A,B). No perturbation of microtubule organisation was evident by either light or electron microscopy. In contrast, CFP:MORN localisation (Fig. 3D,E) and immunofluorescence using 20H5 (data not shown) revealed loss of normal 'bi-lobe' architecture, indicating *Tb*TBCCD1 plays an important role in organising the formation of this structure. A flagellum detachment phenotype in some RNAi-induced cells suggested either (1) synthesis and vesicular trafficking via the Golgi of surface-associated glycoconjugates was potentially affected by loss of bi-lobe organisation – stable attachment of the flagellum to the cell body is dependent upon members of the trypanosomatid-specific FLA1 glycoprotein family (discussed further in Sun et al., 2013; Ginger et al., 2013) – or (2) the flagellar neck region, as well as bi-lobe organisation, was disrupted following RNAi induction, such that flagellum–cell-body attachment at the flagellar pocket exit point could become compromised.

Loss of kinetoplast–basal-body linkage

More striking than losing bi-lobe organisation was the accumulation, post-RNAi induction, of cells either lacking kinetoplasts or possessing abnormally large kinetoplasts (Fig. 3C,G). The kinetoplast is attached to mature and pro-basal bodies by a complex filament-based tripartite attachment complex (TAC) that traverses inner and outer mitochondrial membranes (Ogbadoyi et al., 2003; Jensen and Englund, 2012). Filaments connecting basal body and pro-basal body with the mitochondrial outer membrane are termed exclusion zone filaments, as their presence excludes cytoplasmic ribosomes (Ogbadoyi et al., 2003). The TAC couples basal body segregation with replicated kinetoplast segregation, providing faithful inheritance of single-unit mitochondrial genomes at cytokinesis

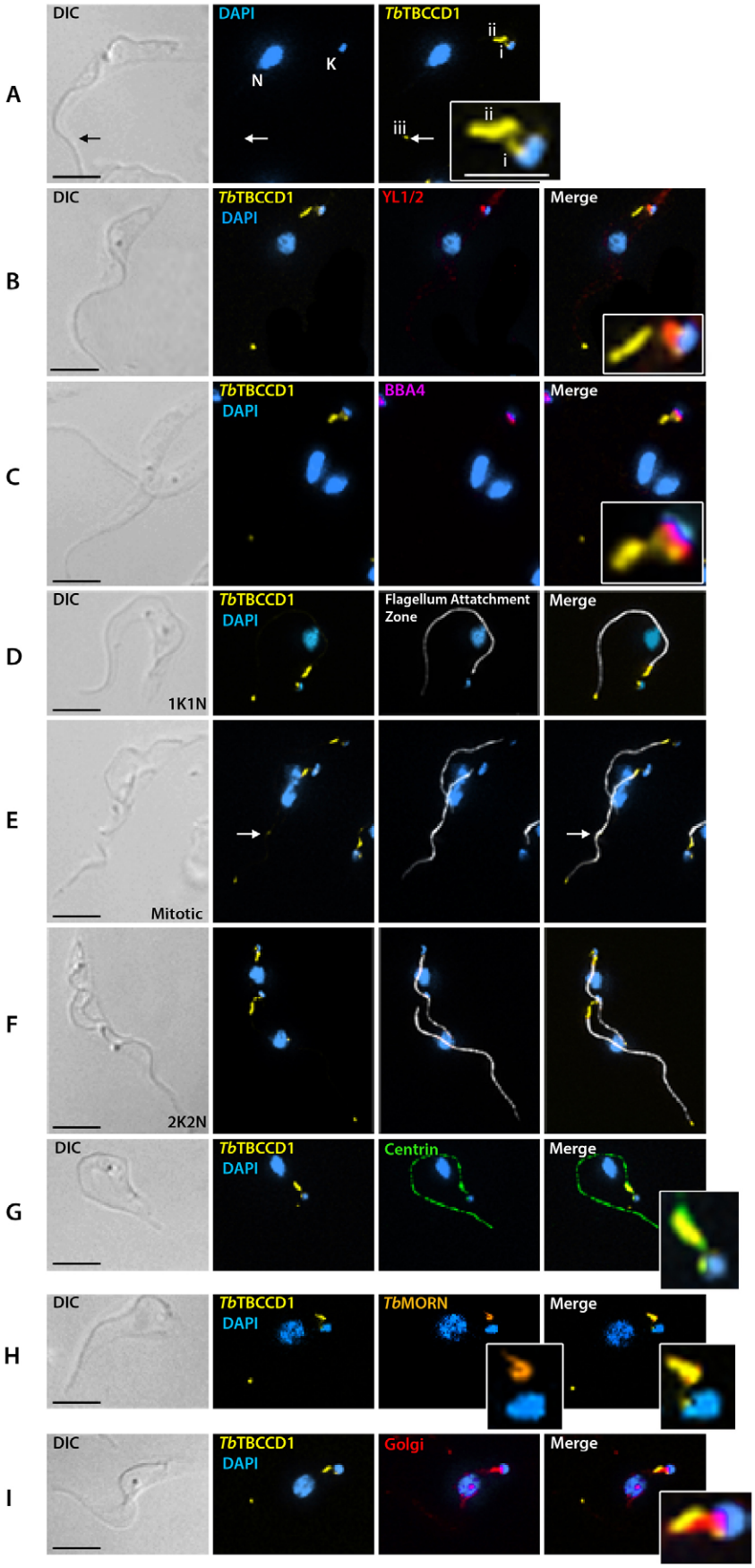

Fig. 1. Localisation of *Tb*TBCCD1. (A) *Tb*TBCCD1 localises to (i) close to the kinetoplast, (ii) an elongate structure immediately anterior to the kinetoplast, and (iii) the anterior end of the cell body (arrowed). K, kinetoplast; N, nucleus. (B,C) Fluorescence labelling experiments with monoclonal antibodies YL1/2 and BBA4 place basal body-localised ^{Ty}YFP:TBCCD1 between markers for the proximal (BBA4) and distal (YL1/2) ends of mature basal bodies; BBA4 colabelling also shows that ^{Ty}YFP:TBCCD1 is localised at the pro-basal body. (D–F) Fluorescence labelling of ^{Ty}YFP:TBCCD1-expressing cells colabelled with L3B2, a monoclonal antibody detecting FAZ1 from the cytoplasmic face of the FAZ. During cell division (E), newly acquired ^{Ty}YFP:TBCCD1 signal (marking the anterior pole of the cell which will inherit the new flagellum; arrowed) is not juxtaposed with the distal end of the FAZ, indicating that the anterior end *Tb*TBCCD1 is acquired before FAZ formation completes. (G,H) Pan-centrin monoclonal antibody 20H5 (G) and a CFP-tagged version of *Tb*MORN (H) identify *Tb*TBCCD1 as a Golgi bi-lobe component. (I) Polyclonal antiserum detecting the Golgi marker RabX2 reveals Golgi stack adjacent to the *Tb*TBCCD1-containing bi-lobe. Inset panels allow closer inspection of colabelling patterns. Scale bars: main panels, 5 μm; insets, 2.5 μm.

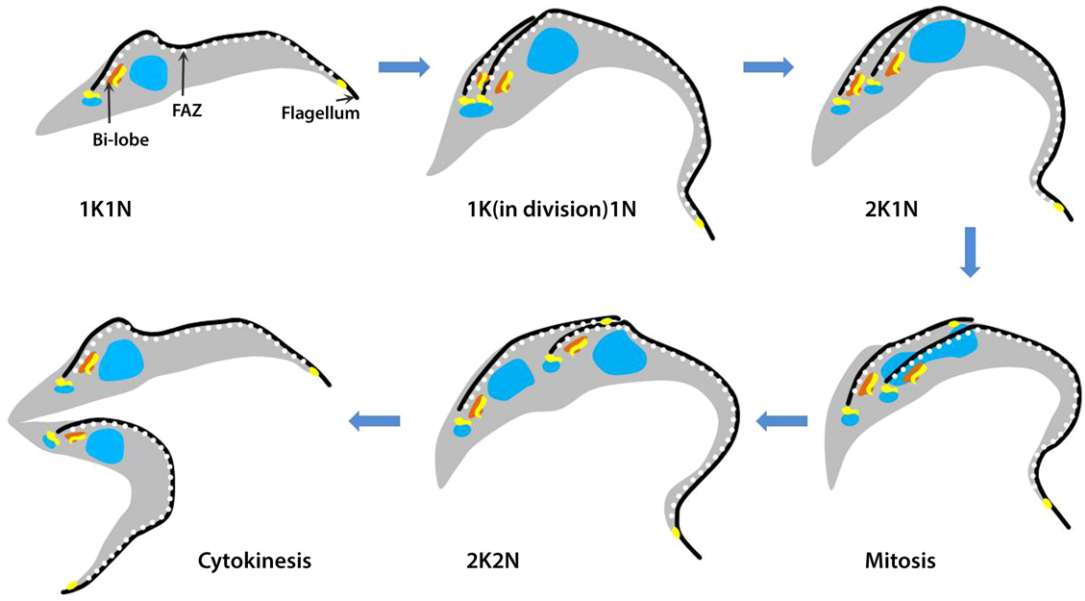

Fig. 2. Illustrations of *Tb*TBCCD1 localisation and duplication. Illustrations of cells from various stages of the cell division cycle showing *Tb*TBCCD1 localisation to the basal or probasal body, Golgi bi-lobe and anterior end of cell body. Nucleus (N), kinetoplast (K), flagellum attachment zone (FAZ) and the Golgi bi-lobe are annotated. Note that in the mitotic cell, new anterior-end *Tb*TBCCD1 signal is acquired before the FAZ has fully matured (as defined by L3B2 labelling), and thus a gap exists between the distal end of the FAZ and the *Tb*TBCCD1 signal. Later in the cell cycle (2K2N) no such gap exists and the *Tb*TBCCD1 signal is juxtaposed with the distal end of the FAZ.

(Robinson and Gull, 1991). Following RNAi induction, in cells with segregated basal bodies but only one kinetoplast, we observed it was the more posterior of the two basal bodies (i.e. the basal body from which the new axoneme extended) that associated with either little or no kinetoplast DNA (kDNA). In these cells, the more anterior basal body was linked to a larger than normal, fluorescence-intense kinetoplast (Fig. 3G); the size and fluorescence intensity of the large kinetoplasts indicated kDNA replication still occurred. Similar increases in kinetoplast size, corresponding to continued kDNA replication were observed in RNAi mutants deficient in mitochondrial TAC components (Zhao et al., 2008; Sykes and Hajduk, 2013). Our observations indicate loss of centriolar *Tb*TBCCD1 causes asymmetric mis-segregation of kDNA.

Given that centriolar *Tb*TBCCD1 lies more distal than antigen recognised by BBA4 (Fig. 1C), *Tb*TBCCD1 would appear unlikely to be an integral component of extra-mitochondrial TAC filaments forming the zone of ribosome exclusion between the proximal end of basal bodies and the underlying mitochondrial membrane (Fig. 4A,B). When RNAi mutants were examined by transmission electron microscopy (TEM), retention of a ribosome exclusion zone beneath akinetoplastic basal bodies was evident (Fig. 4C,D). We suggest that *Tb*TBCCD1 could orchestrate linkage of extra-mitochondrial TAC filaments to mature and pro-basal bodies, thereby mediating a link between the filament-based TAC and the microtubule barrels of pro- and mature basal bodies. Following TbTBCCD1 RNAi induction and an initial round of kinetoplast replication, the posterior mature/pro-basal body pair segregate without attached kDNA. If *Tb*TBCCD1 does link extra-mitochondrial TAC filaments to basal bodies, then retention of a ribosome exclusion zone beneath akinetoplastic basal bodies (Fig. 4C,D) can be explained if TAC nucleation occurs on mitochondrial membranes and proceeds bi-directionally towards the kinetoplast and basal bodies. Alternatively, ultrastructural analyses of diverse trypanosomatids suggest that the TAC architecture is fundamentally conserved throughout the trypanosomatid family (Ogbadoyi et al., 2003; Jensen and Englund, 2012; Souto-Padrón et al., 1984). From the assorted fixations that have informed on TAC architecture, filaments (or fibrils) directly attaching basal bodies to kinetoplasts have been noted in freeze-etch micrographs of the American trypanosome *T. cruzi* (Souto-Padrón et al., 1984). Thus, *Tb*TBCCD1 could be a part of, or orchestrate the formation of, these filaments. Given the complexity of TAC architecture, loss of these filaments might not necessarily prevent the formation of exclusion zone filaments that serve to link basal bodies to the outer mitochondrial membrane, thereby providing another explanation for the retention of exclusion zone filaments beneath akinetoplastic basal bodies.

Detailed analyses of TAC–kinetoplast association are currently limited to mitochondrial proteins (Ochsenreiter et al., 2008; Zhao et al., 2008; Sykes and Hajduk, 2013). We therefore looked further, by using TEM, at the kDNA mis-segregation phenotype arising following RNAi against *Tb*TBCCD1 (a non-mitochondrial, TAC-associated protein). In thin sections from non-induced cultures, basal bodies were always found in association with a kinetoplast (Fig. 4A,B). In contrast, thin sections at 48 hours post-RNAi induction revealed basal bodies associated with no kinetoplast (Fig. 4C,D), or unusually long kinetoplasts with the basal body association to that kinetoplast being generally asymmetric (Fig. 4E). In some cells with unusually long kinetoplasts, ordered stacks of kDNA were observed, specifically in the region lacking an overlying basal body (Fig. 4E,F). The kDNA comprises of two classes of circular DNA: maxi-circles (n=~40) containing protein-coding genes

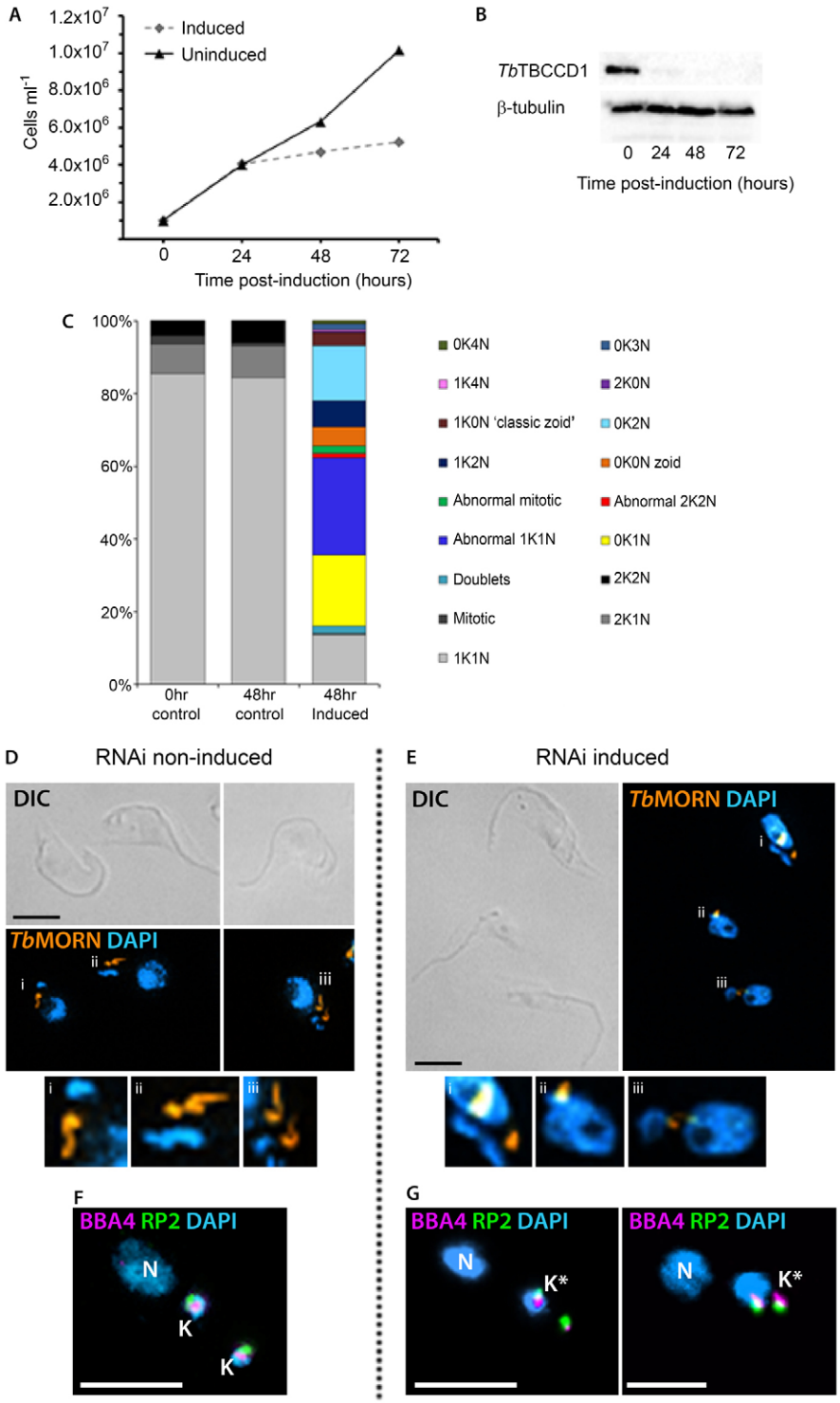

Fig. 3. *Tb*TBCCD1 is an essential protein required for the integrity filament-based trypanosome cytoskeletal structures. (A) Effect of *Tb*TBCCD1 RNAi induction upon trypanosome growth (diamonds) compared to RNAi non-induced control (triangles). (B) Immunoblotting confirms ^{Ty}YFP:TBCCD1 loss post-RNAi induction; KMX1 (specific for β-tubulin) is a loading control. (C) Effect of *Tb*TBCCD1 RNAi induction on kinetoplast and nuclei number, and cell morphology. Zoids are anucleate 'cells'. (D,E) Effect of *Tb*TBCCD1 RNAi induction on the Golgi bi-lobe structure. The distinctive 'fish-hook' CFP:MORN labelling seen in non-induced cells (D) is lost following TbTBCCD1 RNAi induction (E). Inset panels beneath main figures show an enlarged view of the Golgi bi-lobe region in non-induced and induced cells. (F,G) Profound effects of RNAi on kinetoplast segregation. In many biflagellate RNAi-induced cells, the anterior basal body associated with intensely DAPI-stained kDNA but the posterior body was kDNA negative (G). Representative cells shown in F,G were labelled with a polyclonal antiserum recognising *Tb*RP2, denoting transitional fibres at the distal end of mature basal bodies, and BBA4, denoting basal and probasal body proximal ends. N, Nucleus; K, Kinetoplast; K*, replicated un-segregated kinetoplast. Scale bars: 5 μm (main panels in D,E,F,G); 2.5 μm (insets in D,E).

and mini-circles (n=~5000) encoding guide RNAs required for decrypting maxi-circle-derived transcripts. Current kDNA replication models propose that mini-circles move from the kDNA disc into a region situated between the kDNA network and overlying basal body (the kinetoflagellar zone, KFZ; reviewed in Jensen and Englund, 2012). Mini-circle replication occurs within the KFZ, before sister mini-circles migrate to antipodal sites for reattachment to the kDNA periphery. Intriguingly, the presence of electron-lucent regions between well-defined kDNA stacks suggests that despite kinetoplast mis-segregation a structural framework assembles on which replicated kDNA circles then catenate. The electron-lucent regions are potentially analogous to the filament-based KFZ within which mini-circle replication occurs.

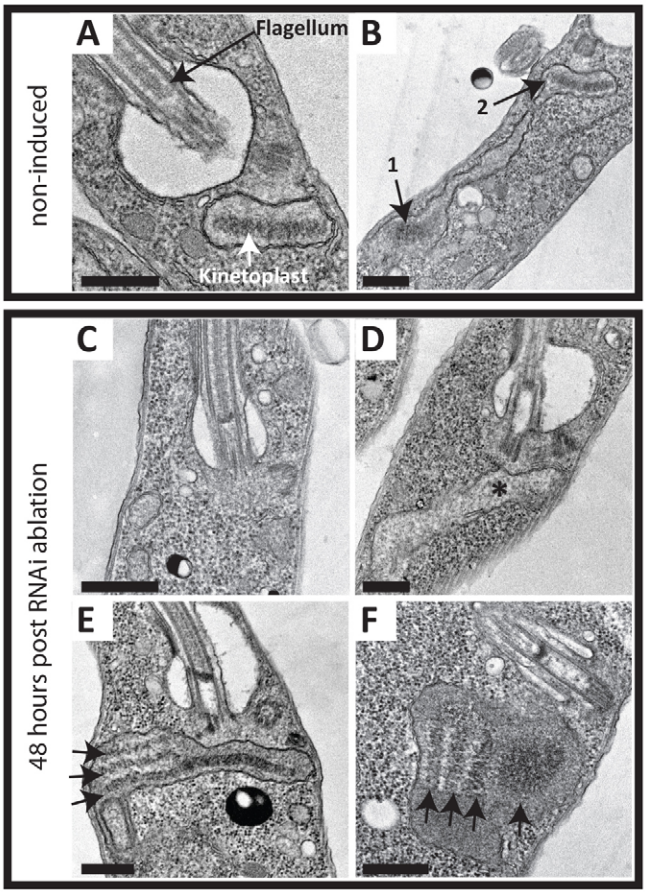

Fig. 4. kDNA mis-segregation and stacking. Thin-section transmission electron micrographs of *Tb*TBCCD1 non-induced (A,B) and RNAi-induced (C–F) cells. (A,B) In non-induced cells, kDNA unmistakably associates with a basal body. In dividing cells (B), the kDNA network segregates due to association (via the TAC) with basal bodies. (C) Following *Tb*TBCCD1 RNAi, kDNA is absent despite the presence of a basal body. kDNA is also absent in the cell shown in D, despite the clear presence of mitochondrial membrane within the plane of sectioning. (E,F) kDNA remaining in association with basal bodies often exhibits stacking (arrows) specifically in regions not associated with basal bodies; electron-lucent regions emphasise the apparently ordered stacking of kDNA. See text for further interpretation of this phenotype. Scale bars: 500 nm.

Zoid formation but no loss of pro-mature basal body linkage

Feldman and Marshall (Feldman and Marshall, 2009) noted TBCCD1 was required for mother–daughter centriole linkage in *Chlamydomonas*. Thus, we asked what effect *Tb*TBCCD1 RNAi had on basal body linkage in trypanosomes. Using BBA4 as an immunofluorescence marker, we saw no evidence for widespread disengagement of pro- and mature basal bodies. Accumulation of anucleate zoids in RNAi-induced populations (Fig. 3C) indicates defects in nuclear positioning following mitosis occur readily. Any filament-based network responsible for nuclear segregation awaits characterisation.

Evolutionary perspectives

The evidence that TBCCD1 is a GAP for either tubulin or another protein is equivocal – the bioinformatic comparison of TBCCD1 orthologues with TBCC and RP2 does not highlight strong conservation of residues linked to GAP activity in XRP2 (our data not shown). Moreover, a variety of experiments reported by Gonçalves et al. (Gonçalves et al., 2010) indicated no direct involvement for human TBCCD1 in microtubule organisation. Gonçalves et al. (Gonçalves et al., 2010) speculated that TBCCD1 could promote crosstalk between the centrosome and actin-based cytoskeleton in mammalian cells. Our data indicate TBCCD1 is involved in filament formation, structures notoriously difficult to visualise by conventional EM approaches. TBCCD1 presence in *Chlamydomonas* rhizoplasts, striated fibres connecting proximal ends of flagellar basal bodies to the nucleus, is consistent with a filament function in this protist, too (and loss of mother–daughter centriole linkage explained by loss of another TBCCD1-dependent filament-based structure). Moreover, TBCCD1–Golgi association is conserved between animals and trypanosomes and probably algae, too (given that rhizoplast–Golgi association has been noted; Brugerolle and Mignot, 2003). The last common ancestor of green algae, trypanosomes and animals was probably the last common ancestor of all eukaryotes (Katz, 2012). A TBCCD1-dependent Golgi-to-centriole or Golgi-to-centrosome linkage has potentially therefore been conserved throughout eukaryotic evolution. Coupled with our unequivocal connection of *Tb*TBCCD1 to two filament-based cytoskeletal structures, it is possible that collectively the available data unexpectedly point to the essential co-option of a key domain required classically in tubulin-folding for a non-tubulin, non-GAP-related function at an early stage in the evolution of the eukaryotic cytoskeleton.

Materials and Methods

Parasite culture

Trypanosomes (SmOxP927; Poon et al., 2012) were cultured in SDM-79 medium supplemented with 10% (v/v) heat-inactivated fetal bovine serum (Brun and Schönenberger, 1979). Stable transformation used standard methods.

Plasmid construction

Fluorescent fusion proteins were expressed using pEnT-based vectors (Kelly et al., 2007). For RNAi, a stem-loop construct (bp 22–1158 of Tb927.11.2440 coding sequence ligated as an inverted repeat to bp 754–25) was cloned between opposing head-to-head T7 RNA polymerase promoters in $p2T7_{177}$ (Wickstead et al., 2002). Primer sequences are available on request. Plasmid sequencing used ABI prism sequencing technology.

Immunofluorescence and immunoblotting

Cells were settled onto coverslips and either fixed directly with 3.7% paraformaldehyde or detergent-extracted for 45 seconds with 1% Nonidet-P40 in 0.1M PIPES pH 6.9, 2 mM EGTA, 1 mM $MgSO_4$ and 0.1 mM EDTA, prior to fixation. Processing continued with a 10-minute incubation in −20℃ methanol, followed by rehydration in phosphate-buffered saline (PBS). *Tb*RP2-specific polyclonal antiserum (prepared by Eurogentech and affinity-purified) was used at 1:50 dilution with a 1% BSA block (immunofluorescence) or 1:100 with 1% Marvel block (immunoblotting). Immunofluorescence with monoclonal antibodies YL1/2 (Kilmartin et al., 1982), BBA4 (Woodward et al., 1995), L3B2 (Vaughan et al., 2008), RabX2 (Natesan et al., 2009) and 20H5 (Millipore) was performed as described previously or following supplier's instructions (20H5). Images were captured and processed using an Applied Precision DeltaVision Deconvolution microscope system and SoftWoRx software. Nuclei and kinetoplast counts were determined using a Leica DM RXA2 microscope and associated FW4000 software. Immunoblotting using BB2 was as described previously (Bastin et al., 1996).

Electron microscopy

Fixation was by addition of glutaraldehyde (2.5% final concentration, 5 minutes) to cultures. Cell pellets were re-suspended in 0.1M PBS (pH 7.4) for 10 minutes, followed by 2.5% glutaraldehyde, 2% paraformaldehyde and 0.1% tannic acid in 0.1M phosphate buffer (pH 7.0) for 2 hours at room temperature. Pellets were washed with 0.1 M phosphate buffer (pH 7.0) and post-fixed in 1% osmium tetroxide in 0.1M phosphate buffer (pH 7.0) for 1 hour at room temperature. Samples were rinsed and stained en bloc for 40 minutes in 2% uranyl acetate,

dehydrated in an ascending acetone series and embedded in Agar 100 resin (Agar Scientific). Random thin-section electron microscopy was performed using a Hitachi H-7650, operated at 120 kV.

Bioinformatics

Protein sequences were aligned by Clustal Omega (Sievers et al., 2011) and secondary structure predictions were carried out using Phyre^2 (Kelley and Sternberg, 2009).

Acknowledgements

We thank Keith Gull (University of Oxford, UK) for kindly providing the monoclonal antibodies BBA4 and L3B2 and Mark Field (University of Cambridge, UK) for the polyclonal antiserum recognising RabX2.

Author contributions

P.G.M. and M.L.G. designed the research. J.A., S.H. and X.Q., contributed to the generation of mutants and light microscopy experiments. K.T. and S.V. analysed mutant cells by TEM. J.A., S.V., P.G.M. and M.L.G. wrote the manuscript.

Funding

This work was supported by grants from the Biotechnology and Biological Sciences Research Council (BBSRC) [grant numbers BBG0210581, BBF0109311 to P.G.M. and M.L.G., and BB/1000402/1 to S.V.]. Deposited in PMC for release after 6 months.

References

Bartolini, F., Bhamidipati, A., Thomas, S., Schwahn, U., Lewis, S. A. and Cowan, N. J. (2002). Functional overlap between retinitis pigmentosa 2 protein and the tubulin-specific chaperone cofactor C. *J. Biol. Chem.* **277**, 14629-14634.

Bastin, P., Bagherzadeh, Z., Matthews, K. R. and Gull, K. (1996). A novel epitope tag system to study protein targeting and organelle biogenesis in Trypanosoma brucei. *Mol. Biochem. Parasitol.* **77**, 235-239.

Brugerolle, G. and Mignot, J. P. (2003). The rhizoplast of chrysomonads, a basal body-nucleus connector that polarises the dividing spindle. *Protoplasma* **222**, 13-21.

Brun, R. and Schönenberger, M. (1979). Cultivation and in vitro cloning or procyclic culture forms of Trypanosoma brucei in a semi-defined medium. Short communication. *Acta Trop.* **36**, 289-292.

Esson, H. J., Morriswood, B., Yavuz, S., Vidilaseris, K., Dong, G. and Warren, G. (2012). Morphology of the trypanosome bilobe, a novel cytoskeletal structure. *Eukaryot. Cell* **11**, 761-772.

Feldman, J. L. and Marshall, W. F. (2009). ASQ2 encodes a TBCC-like protein required for mother-daughter centriole linkage and mitotic spindle orientation. *Curr. Biol.* **19**, 1238-1243.

Gheiratmand, L., Brasseur, A., Zhou, Q. and He, C. Y. (2013). Biochemical characterization of the bi-lobe reveals a continuous structural network linking the bi-lobe to other single-copied organelles in Trypanosoma brucei. *J. Biol. Chem.* **288**, 3489-3499.

Ginger, M. L., Collingridge, P. W., Brown, R. W. B., Sproat, R., Shaw, M. K. and Gull, K. (2013). Calmodulin is required for paraflagellar rod assembly and flagellum-cell body attachment in trypanosomes. *Protist* **164**, 528-540.

Gonçalves, J., Nolasco, S., Nascimento, R., Lopez Fanarraga, M., Zabala, J. C. and Soares, H. (2010). TBCCD1, a new centrosomal protein, is required for centrosome and Golgi apparatus positioning. *EMBO Rep.* **11**, 194-200.

Ho, H. H., He, C. Y., de Graffenried, C. L., Murrells, L. J. and Warren, G. (2006). Ordered assembly of the duplicating Golgi in Trypanosoma brucei. *Proc. Natl. Acad. Sci. USA* **103**, 7676-7681.

Jensen, R. E. and Englund, P. T. (2012). Network news: the replication of kinetoplast DNA. *Annu. Rev. Microbiol.* **66**, 473-491.

Katz, L. A. (2012). Origin and diversification of eukaryotes. *Annu. Rev. Microbiol.* **66**, 411-427.

Kelley, L. A. and Sternberg, M. J. E. (2009). Protein structure prediction on the Web: a case study using the Phyre server. *Nat. Protoc.* **4**, 363-371.

Kelly, S., Reed, J., Kramer, S., Ellis, L., Webb, H., Sunter, J., Salje, J., Marinsek, N., Gull, K., Wickstead, B. et al. (2007). Functional genomics in Trypanosoma brucei: a collection of vectors for the expression of tagged proteins from endogenous and ectopic gene loci. *Mol. Biochem. Parasitol.* **154**, 103-109.

Kilmartin, J. V., Wright, B. and Milstein, C. (1982). Rat monoclonal antitubulin antibodies derived by using a new nonsecreting rat cell line. *J. Cell Biol.* **93**, 576-582.

Kühnel, K., Veltel, S., Schlichting, I. and Wittinghofer, A. (2006). Crystal structure of the human retinitis pigmentosa 2 protein and its interaction with Arl3. *Structure* **14**, 367-378.

Morriswood, B., Havlicek, K., Demmel, L., Yavuz, S., Sealey-Cardona, M., Vidilaseris, K., Anrather, D., Kostan, J., Djinovic-Carugo, K., Roux, K. J. et al. (2013). Novel bilobe components in Trypanosoma brucei identified using proximity-dependent biotinylation. *Eukaryot. Cell* **12**, 356-367.

Natesan, S. K., Peacock, L., Leung, K. F., Matthews, K. R., Gibson, W. and Field, M. C. (2009). The trypanosome Rab-related proteins RabX1 and RabX2 play no role in intracellular trafficking but may be involved in fly infectivity. *PLoS ONE* **4**, e7217.

Ochsenreiter, T., Anderson, S., Wood, Z. A. and Hajduk, S. L. (2008). Alternative RNA editing produces a novel protein involved in mitochondrial DNA maintenance in trypanosomes. *Mol. Cell. Biol.* **28**, 5595-5604.

Ogbadoyi, E., Ersfeld, K., Robinson, D., Sherwin, T. and Gull, K. (2000). Architecture of the Trypanosoma brucei nucleus during interphase and mitosis. *Chromosoma* **108**, 501-513.

Ogbadoyi, E. O., Robinson, D. R. and Gull, K. (2003). A high-order trans-membrane structural linkage is responsible for mitochondrial genome positioning and segregation by flagellar basal bodies in trypanosomes. *Mol. Biol. Cell* **14**, 1769-1779.

Poon, S. K., Peacock, L., Gibson, W., Gull, K. and Kelly, S. (2012). A modular and optimized single marker system for generating Trypanosoma brucei cell lines expressing T7 RNA polymerase and the tetracycline repressor. *Open Biol.* **2**, 110037.

Portman, N. and Gull, K. (2012). Proteomics and the Trypanosoma brucei cytoskeleton: advances and opportunities. *Parasitology* **139**, 1168-1177.

Robinson, D. R. and Gull, K. (1991). Basal body movements as a mechanism for mitochondrial genome segregation in the trypanosome cell cycle. *Nature* **352**, 731-733.

Schwarz, N., Novoselova, T. V., Wait, R., Hardcastle, A. J. and Cheetham, M. E. (2012). The X-linked retinitis pigmentosa protein RP2 facilitates G protein traffic. *Hum. Mol. Genet.* **21**, 863-873.

Sherwin, T. and Gull, K. (1989). The cell division cycle of Trypanosoma brucei brucei: timing of event markers and cytoskeletal modulations. *Philos. Trans. R. Soc. B* **323**, 573-588.

Sievers, F., Wilm, A., Dineen, D., Gibson, T. J., Karplus, K., Li, W., Lopez, R., McWilliam, H., Remmert, M., Söding, J. et al. (2011). Fast, scalable generation of high-quality protein multiple sequence alignments using Clustal Omega. *Mol. Syst. Biol.* **7**, 539.

Souto-Padrón, T., de Souza, W. and Heuser, J. E. (1984). Quick-freeze, deep-etch rotary replication of Trypanosoma cruzi and Herpetomonas megaseliae. *J. Cell Sci.* **69**, 167-178.

Stephan, A., Vaughan, S., Shaw, M. K., Gull, K. and McKean, P. G. (2007). An essential quality control mechanism at the eukaryotic basal body prior to intraflagellar transport. *Traffic* **8**, 1323-1330.

Sun, S. Y., Wang, C., Yuan, Y. A. and He, C. Y. (2013). An intracellular membrane junction consisting of flagellum adhesion glycoproteins links flagellum biogenesis to cell morphogenesis in Trypanosoma brucei. *J. Cell Sci.* **126**, 520-531.

Sykes, S. E. and Hajduk, S. L. (2013). Dual functions of α-ketoglutarate dehydrogenase E2 in the Krebs cycle and mitochondrial DNA inheritance in Trypanosoma brucei. *Eukaryot. Cell* **12**, 78-90.

Tian, G., Huang, Y., Rommelaere, H., Vandekerckhove, J., Ampe, C. and Cowan, N. J. (1996). Pathway leading to correctly folded beta-tubulin. *Cell* **86**, 287-296.

Vaughan, S., Kohl, L., Ngai, I., Wheeler, R. J. and Gull, K. (2008). A repetitive protein essential for the flagellum attachment zone filament structure and function in Trypanosoma brucei. *Protist* **159**, 127-136.

Veltel, S., Gasper, R., Eisenacher, E. and Wittinghofer, A. (2008). The retinitis pigmentosa 2 gene product is a GTPase-activating protein for Arf-like 3. *Nat. Struct. Mol. Biol.* **15**, 373-380.

Wickstead, B., Ersfeld, K. and Gull, K. (2002). Targeting of a tetracycline-inducible expression system to the transcriptionally silent minichromosomes of Trypanosoma brucei. *Mol. Biochem. Parasitol.* **125**, 211-216.

Woods, A., Sherwin, T., Sasse, R., MacRae, T. H., Baines, A. J. and Gull, K. (1989). Definition of individual components within the cytoskeleton of Trypanosoma brucei by a library of monoclonal antibodies. *J. Cell Sci.* **93**, 491-500.

Woodward, R., Carden, M. J. and Gull, K. (1995). Immunological characterization of cytoskeletal proteins associated with the basal body, axoneme and flagellum attachment zone of Trypanosoma brucei. *Parasitology* **111**, 77-85.

Zhao, Z., Lindsay, M. E., Roy Chowdhury, A., Robinson, D. R. and Englund, P. T. (2008). p166, a link between the trypanosome mitochondrial DNA and flagellum, mediates genome segregation. *EMBO J.* **27**, 143-154.